Supplementary information for "Characterization of collective excitations in weakly-coupled disordered superconductors"

Bo Fan,[1,*] Abhisek Samanta,[2,†] and Antonio M. García-García[1,‡]

[1] *Shanghai Center for Complex Physics, School of Physics and Astronomy, Shanghai Jiao Tong University, Shanghai 200240, China*

[2] *Physics Department, Technion, Haifa 32000, Israel*

This supplemental information is divided into three sections. We first provide all the technical details necessary to compute the full current-current correlator that enter in the definition of the ac conductivity. In section II, we study the collective modes by computing the phase and amplitude spectral function in different cases. Section III contains results for the phase fluctuation correlation functions and the optical conductivity not presented in the main text.

I. CURRENT-CURRENT CORRELATORS IN DISORDERED SUPERCONDUCTORS

We consider a disordered attractive Hubbard model on a square lattice in presence of onsite random potential V_i ($V_i \in [-V, V]$). The model Hamiltonian is given by,

$$H = -t \sum_{\langle ij \rangle \sigma} c^\dagger_{i\sigma} c_{j\sigma} - U \sum_i n_{i\uparrow} n_{i\downarrow} + \sum_i V_i n_i \tag{S1}$$

where t is the hopping amplitude between two nearest neighbors, and U is the attractive interaction responsible for the Cooper pairing. A first step of the calculation is to write down the inhomogeneous mean-field Hamiltonian. For that purpose, we employ the standard Bogoliubov de-Gennes [1, 2] theory with two mean-field parameters: local superconducting order parameter $\Delta(i)$ and local density $n(i)$ [3, 4]. We then use the following Bogoliubov transformation,

$$c_{i\sigma} = \sum_n \left(u_n(i)\gamma_{n\sigma} - \sigma v^*_n(i)\gamma^\dagger_{n\bar{\sigma}} \right) \tag{S2}$$

which diagonalizes the effective mean-field Hamiltonian in a fermionic quasi-particle basis (γ),

$$H_{MF} = \sum_{n\sigma} E_n \gamma^\dagger_{n\sigma}\gamma_{n\sigma}, \tag{S3}$$

where n runs over the positive eigenvalues i.e. $E_n > 0$.

Next, we study the effect of disorder on the optical response of the system. The dynamical correlation function is given by [5],

$$\chi_{ij}(\phi, \phi') = -i \int dt e^{i\omega t} \langle [\phi_i(t),\ \phi'_j(0)] \rangle \tag{S4}$$

where ϕ corresponds to the fluctuation components and the current operators [5],

$$\begin{aligned} \delta\Delta_i &= c_{i\downarrow}c_{i\uparrow} - \langle c_{i\downarrow}c_{i\uparrow}\rangle \\ \delta\Delta^\dagger_i &= c^\dagger_{i\uparrow}c^\dagger_{i\downarrow} - \langle c^\dagger_{i\uparrow}c^\dagger_{i\downarrow}\rangle \\ \delta n_i &= \sum_\sigma \left(c^\dagger_{i\sigma}c_{i\sigma} - \langle c^\dagger_{i\sigma}c_{i\sigma}\rangle \right) \\ j^\alpha_i &= it \sum_\sigma \left(c^\dagger_{i+\alpha,\sigma}c_{i\sigma} - c^\dagger_{i\sigma}c_{i+\alpha,\sigma} \right). \end{aligned} \tag{S5}$$

Here $\delta\Delta_i$ is the fluctuation in local superconducting order parameter, and δn_i is the fluctuation in local density. $\langle \cdots \rangle$ corresponds to the expectation value of the operator in the inhomogeneous BdG eigenstate. The amplitude fluctuation A_i and the phase fluctuation Φ_i of the superconducting order parameter are defined by

$$A_i = (\delta\Delta_i + \delta\Delta^\dagger_i)/\sqrt{2} \tag{S6}$$

$$\Phi_i = i(\delta\Delta_i - \delta\Delta^\dagger_i)/\sqrt{2} \tag{S7}$$

Note that all the eigenvectors (u_n, v_n) in our case are real. Hence, we can express the dynamical correlation functions only in terms of the outcome of the Bogoliubov-deGennes mean field formalism: u_n, v_n and E_n only. That enables us to write down explicit expressions for the different correlation functions at zero temperature in terms of these quantities.

For instance, the bare current-current correlation function, directly relevant in the calculation of the conductivity, is given by [3],

$$\chi^0_{ij}(j^x, j^x) = 2t^2 \sum_{nm} \left(v_m(j+\hat{x})u_n(j) + v_n(j+\hat{x})u_m(j)\right) \left(\frac{u_n(i+\hat{x})v_m(i) - u_n(i)v_m(i+\hat{x})}{i\omega_p + E_n + E_m} - \frac{v_n(i)u_m(i+\hat{x}) - v_n(i+\hat{x})u_m(i)}{i\omega_p - E_n - E_m} \right) + u \leftrightarrow v \tag{S8}$$

where $i\omega_p$ is the bosonic Matsubara frequency $\omega_p = 2\pi p/\beta$.

The full [5] gauge invariant current-current correlation function, including vertex corrections that restore gauge invariance, is given by,

$$\chi_{ij}\left(j^x, j^x\right) = \chi^0_{ij}\left(j^x, j^x\right) + \Lambda_{ip} \mathbb{V}_{pl} \left(\mathbb{I}_{3N\times 3N} - \chi^B \mathbb{V}\right)^{-1}_{ls} \bar{\Lambda}_{sj} \tag{S9}$$

where $i, j, p, l, s = 1, \ldots N$ are site indexes, χ^0 is the bare current-current correlation function, sum over repeated indexes is understood, and Λ couples the current with the fluctuations of the amplitude A, phase Φ and charge density δn,

$$\Lambda = \begin{pmatrix} \chi(j^x, A) & \chi(j^x, \Phi) & \chi(j^x, \delta n) \end{pmatrix} \tag{S10}$$

$$\bar{\Lambda} = \begin{pmatrix} \chi(A, j^x) & \chi(\Phi, j^x) & \chi(\delta n, j^x) \end{pmatrix}^T . \tag{S11}$$

χ^B, the bare mean-field susceptibility and $\mathbb{V}$, the effective local interaction, are 3×3 matrices in the basis of fluctuations:

$$\chi^B = \begin{pmatrix} \chi(A, A) & \chi(A, \Phi) & \chi(A, \delta n) \\ \chi(\Phi, A) & \chi(\Phi, \Phi) & \chi(\Phi, \delta n) \\ \chi(\delta n, A) & \chi(\delta n, \Phi) & \chi(\delta n, \delta n) \end{pmatrix} \tag{S12}$$

and

$$\mathbb{V} = \begin{pmatrix} -|U| & 0 & 0 \\ 0 & -|U| & 0 \\ 0 & 0 & -|U|/2 \end{pmatrix} . \tag{S13}$$

Therefore, in Eqn. (S9), for example, $\chi^B(A, A) = \chi^{AA}$, $\mathbb{V}^A = -|U|\mathbb{I}_{\mathbb{N}\times\mathbb{N}}$ and so on. Note that all of them are $N \times N$ matrices in real space where N is the number of sites in one direction. For the sake of clarity, we depict in Fig. S1 an explicit diagrammatic representation of the gauge invariant current-current correlation function Eq. (S9).

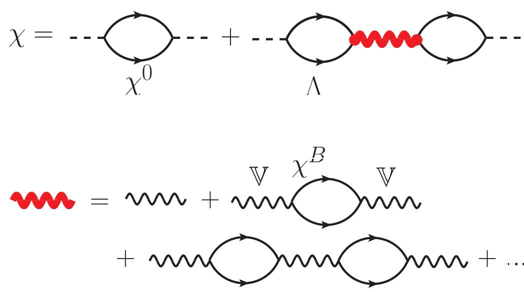

$$= \mathbb{V} + \mathbb{V}\chi^B\mathbb{V} + \mathbb{V}\chi^B\mathbb{V}\chi^B\mathbb{V} + \ldots$$
$$= \mathbb{V} + \mathbb{V}\tilde{\chi}^B\mathbb{V}$$

Figure S1. Diagrammatic representation of the full gauge-invariant current-current correlation function Eq. (S9). Here χ^0 corresponds to the bare current-current correlation function. The solid lines represent superconducting Nambu Green functions, while the dashed lines connecting it represent electromagnetic field. This "bare-bubble" diagram contributes to the optical conductivity above the spectral gap. The RPA vertex correction added to the optical conductivity is represented by the wavy line (red), which includes different fluctuations around the mean-field order parameter. χ^B represents the correlation function between different fluctuation components (leading to the collective modes) (Eq. (S12)), and the correlation function Λ couples current to the collective modes (Eq. (S11)) via the interaction matrix $\mathbb{V}$ (Eq. (S13)). Physically, the Cooper pairs are broken by the incoming electromagnetic field, and the vertex corrections correspond to the exchange of collective excitations between them. Therefore, this contributes to sub-gap optical conductivity in our calculation.

Finally, we provide explicit expressions for all bare components of the Λ and χ^B matrices above. For convenience, we drop the B superscript and start with the expressions of the bare susceptibilities in a different basis describing the correlations between the current operator and the pair fluctuations $(\delta\Delta^\dagger, \delta\Delta)$, or the charge density fluctuations (δn),

$$\chi_{ij}(j^x, \delta\Delta) = 2it \sum_{nm} \left(u_n(i+\hat{x})v_m(i) - u_n(i)v_m(i+\hat{x})\right) \left(\frac{u_m(j)u_n(j)}{i\omega_p + E_n + E_m} - \frac{v_m(j)v_n(j)}{i\omega_p - E_n - E_m}\right) \tag{S14}$$

$$\chi_{ij}(j^x, \delta\Delta^\dagger) = -2it \sum_{nm} \left(u_n(i+\hat{x})v_m(i) - u_n(i)v_m(i+\hat{x})\right) \left(\frac{v_m(j)v_n(j)}{i\omega_p + E_n + E_m} - \frac{u_m(j)u_n(j)}{i\omega_p - E_n - E_m}\right) \tag{S15}$$

$$\begin{aligned}\chi_{ij}(j^x, \delta n) = 2it \sum_{nm} &- \frac{\left(u_n(i+\hat{x})v_m(i) - u_n(i)v_m(i+\hat{x})\right)\left(v_m(j)u_n(j) + v_n(j)u_m(j)\right)}{i\omega_p + E_n + E_m} \\ &+ \frac{\left(v_n(i+\hat{x})u_m(i) - v_n(i)u_m(i+\hat{x})\right)\left(u_m(j)v_n(j) + u_n(j)v_m(j)\right)}{i\omega_p - E_n - E_m}\end{aligned} \tag{S16}$$

The bare correlation functions between pair fluctuations $(\delta\Delta^\dagger, \delta\Delta)$ and charge density fluctuations (δn) are given by,

$$\chi_{ij}(\delta\Delta, \delta\Delta) = \sum_{nm} -\frac{u_n(i)u_m(i)v_m(j)v_n(j)}{i\omega_p - E_n - E_m} + \frac{v_n(i)v_m(i)u_m(j)u_n(j)}{i\omega_p + E_n + E_m} \tag{S17}$$

$$\chi_{ij}(\delta\Delta, \delta\Delta^\dagger) = \sum_{nm} \frac{u_n(i)u_m(i)u_m(j)u_n(j)}{i\omega_p - E_n - E_m} - \frac{v_n(i)v_m(i)v_m(j)v_n(j)}{i\omega_p + E_n + E_m} \tag{S18}$$

$$\chi_{ij}(\delta\Delta^\dagger, \delta\Delta) = \sum_{nm} \frac{v_n(i)v_m(i)v_m(j)v_n(j)}{i\omega_p - E_n - E_m} - \frac{u_n(i)u_m(i)u_m(j)u_n(j)}{i\omega_p + E_n + E_m} \tag{S19}$$

$$\chi_{ij}(\delta\Delta, \delta n) = -2 \sum_{nm} \frac{u_n(i)u_m(i)u_m(j)v_n(j)}{i\omega_p - E_n - E_m} + \frac{v_n(i)v_m(i)v_m(j)u_n(j)}{i\omega_p + E_n + E_m} \tag{S20}$$

$$\chi_{ij}(\delta n, \delta\Delta) = 2 \sum_{nm} \frac{u_n(i)v_m(i)u_m(j)u_n(j)}{i\omega_p + E_n + E_m} + \frac{v_n(i)u_m(i)v_m(j)v_n(j)}{i\omega_p - E_n - E_m} \tag{S21}$$

$$\chi_{ij}(\delta n, \delta n) = 2 \sum_{nm} \left(v_m(j)u_n(j) + v_n(j)u_m(j)\right) \left(-\frac{u_n(i)v_m(i)}{i\omega_p + E_n + E_m} + \frac{v_m(i)u_n(i)}{i\omega_p - E_n - E_m}\right) \tag{S22}$$

The remaining correlation functions are obtained by using symmetry arguments,

$$\begin{aligned}
\chi_{ij}(\Delta, j^x) &= -\chi_{ji}(j^x, \Delta^\dagger)\\
\chi_{ij}(\Delta^\dagger, j^x) &= -\chi_{ji}(j^x, \Delta)\\
\chi_{ij}(n, j^x) &= -\chi_{ji}(j^x, n)\\
\chi_{ij}(\Delta^\dagger, \Delta^\dagger) &= \chi_{ji}(\Delta, \Delta)\\
\chi_{ij}(\Delta^\dagger, n) &= \chi_{ji}(n, \Delta)\\
\chi_{ij}(n, \Delta^\dagger) &= \chi_{ji}(\Delta, n)
\end{aligned} \tag{S23}$$

With the definitions of amplitude and phase fluctuations given in Eqn. (S6) and (S7), we now write down explicitly the bare susceptibilities that enter in the full expression for the current-current susceptibitility Eq. (S9), including vertex corrections, that involves correlations between current and amplitude or phase fluctuations,

$$\chi_{ij}(j^x, A) \;=\frac{1}{\sqrt{2}}\left(\chi_{ij}(j^x, \delta\Delta) + \chi_{ij}(j^x, \delta\Delta^\dagger)\right) \tag{S24}$$

$$\chi_{ij}(A, j^x) \;=\frac{1}{\sqrt{2}}\left(\chi_{ij}(\delta\Delta, j^x) + \chi_{ij}(\delta\Delta^\dagger, j^x)\right) \tag{S25}$$

$$\chi_{ij}(j^x, \Phi) \;=\frac{i}{\sqrt{2}}\left(\chi_{ij}(j^x, \delta\Delta) - \chi_{ij}(j^x, \delta\Delta^\dagger)\right) \tag{S26}$$

$$\chi_{ij}(\Phi, j^x) =\frac{i}{\sqrt{2}}\left(\chi_{ij}(\delta\Delta, j^x) - \chi_{ij}(\delta\Delta^\dagger, j^x)\right), \tag{S27}$$

and correlations between amplitude fluctuation, phase fluctuation and density fluctuation,

$$\chi_{ij}(A, A)= \frac{1}{2}\left[\chi_{ij}(\delta\Delta, \delta\Delta) + \chi_{ij}(\delta\Delta, \delta\Delta^\dagger) + \chi_{ij}(\delta\Delta^\dagger, \delta\Delta) + \chi_{ij}(\delta\Delta^\dagger, \delta\Delta^\dagger)\right] \tag{S28}$$

$$\chi_{ij}(A, \Phi)= \frac{i}{2}\left[\chi_{ij}(\delta\Delta, \delta\Delta) - \chi_{ij}(\delta\Delta, \delta\Delta^\dagger) + \chi_{ij}(\delta\Delta^\dagger, \delta\Delta) - \chi_{ij}(\delta\Delta^\dagger, \delta\Delta^\dagger)\right] \tag{S29}$$

$$\chi_{ij}(A, \delta n)= \frac{1}{\sqrt{2}}\left[\chi_{ij}(\delta\Delta, \delta n) + \chi_{ij}(\delta\Delta^\dagger, \delta n)\right] \tag{S30}$$

$$\chi_{ij}(\Phi, A)= \frac{i}{2}\left[\chi_{ij}(\delta\Delta, \delta\Delta) + \chi_{ij}(\delta\Delta, \delta\Delta^\dagger) - \chi_{ij}(\delta\Delta^\dagger, \delta\Delta) - \chi_{ij}(\delta\Delta^\dagger, \delta\Delta^\dagger)\right] \tag{S31}$$

$$\chi_{ij}(\Phi, \Phi)= \frac{i^2}{2}\left[\chi_{ij}(\delta\Delta, \delta\Delta) - \chi_{ij}(\delta\Delta, \delta\Delta^\dagger) - \chi_{ij}(\delta\Delta^\dagger, \delta\Delta) + \chi_{ij}(\delta\Delta^\dagger, \delta\Delta^\dagger)\right] \tag{S32}$$

$$\chi_{ij}(\Phi, \delta n)= \frac{i}{\sqrt{2}}\left[\chi_{ij}(\delta\Delta, \delta n) - \chi_{ij}(\delta\Delta^\dagger, \delta n)\right] \tag{S33}$$

$$\chi_{ij}(\delta n, A)= \frac{1}{\sqrt{2}}\left[\chi_{ij}(\delta n, \delta\Delta) + \chi_{ij}(\delta n, \delta\Delta^\dagger)\right] \tag{S34}$$

$$\chi_{ij}(\delta n, \Phi)= \frac{i}{\sqrt{2}}\left[\chi_{ij}(\delta n, \delta\Delta) - \chi_{ij}(\delta n, \delta\Delta^\dagger)\right]. \tag{S35}$$

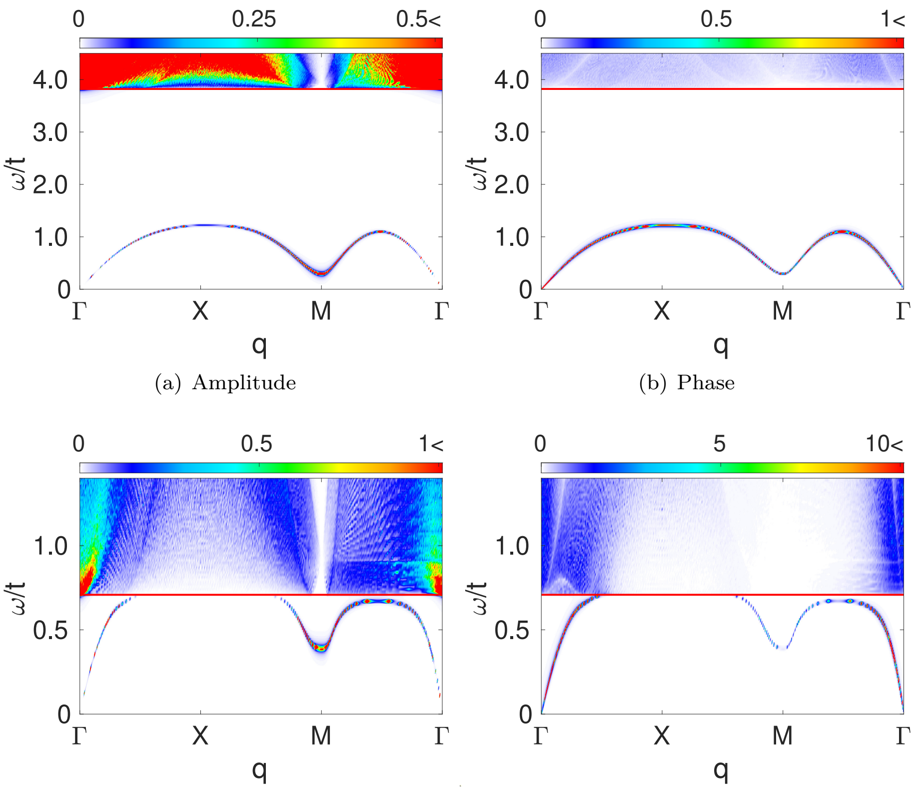

(a) Amplitude (b) Phase

(c) Amplitude (d) Phase

Figure S2. Amplitude ($P^A(q,\omega)$) and phase ($P^\Phi(q,\omega)$) spectral functions for two different couplings U in the clean limit i.e. $V=0$, as a function of momenta q (i.e. $\Gamma(0,0)$, $X(\pi,0)$, and $M(\pi,\pi)$ in momentum space). The figures show the low-energy dispersing collective modes, as well as the two-particle continuum above the spectral gap ω_g (the red horizontal line). The upper panel is for $U=5$, and the lower panel is for $U=2$. The system size is 200×200 and the average density is $\langle n\rangle = 0.875$.

II. CHARACTERIZATION OF COLLECTIVE MODES BY SPECTRAL FUNCTIONS

To study the collective modes, we construct the following matrix in real space

$$\tilde{\chi}^B = \left(\mathbb{I}_{3N\times 3N} - \chi^B \mathbb{V}\right)^{-1}\chi^B = \begin{pmatrix} \tilde{\chi}^{AA} & \tilde{\chi}^{A\Phi} & \tilde{\chi}^{A\delta n} \\ \tilde{\chi}^{\Phi A} & \tilde{\chi}^{\Phi\Phi} & \tilde{\chi}^{\Phi\delta n} \\ \tilde{\chi}^{\delta n A} & \tilde{\chi}^{\delta n\Phi} & \tilde{\chi}^{\delta n\delta n} \end{pmatrix} \tag{S36}$$

to obtain the amplitude spectral function $P^A_{ij}(\omega) = -\frac{1}{\pi}\tilde{\chi}^{AA}_{ij}(\omega)$ and phase spectral function $P^\Phi_{ij}(\omega) = -\frac{1}{\pi}\tilde{\chi}^{\Phi\Phi}_{ij}(\omega)$. Then, we do Fourier transformation to get the $P^A(q,\omega)$ and $P^\Phi(q,\omega)$, to observe the behaviour of amplitude and phase collective modes in momentum space.

In the clean limit, we clearly see collective modes in the phase sector with a linear dispersion relation $\omega \propto q$, which corresponds to the gapless Goldstone mode, see Fig. S2. By contrast, collective modes in the amplitude (the Higgs mode) have a finite gap ω_H [6]. In the $q\to 0$ limit, the gap ω_H is the same as the two-particle gap ω_g. In the strong coupling limit, the collective modes are well below the two-particle gap. However, as the coupling $|U|$ decreases, the two-particle gap reduces as well thus making the collective modes difficult to observe. The same conclusion also holds as the average density $\langle n\rangle$ decreases.

In the weak disorder region, in addition to the dispersing collective modes, a non-dispersive mode appears in the amplitude sector at finite energy below the two-particle continuum, which has been recently identified as the *disorder-induced Higgs mode* [6], see Fig. S3. On the other hand, the phase mode remains dispersing, but gets broadened. In the strong coupling limit, these modifications are easier to observe as the collective mode remains well below the two-particle spectral gap. When disorder becomes large, the *disorder-induced Higgs mode* gets broadened in energy and hence gets mixed with the incoherent spectral weight coming down from two-particle continuum which makes hard to identify it. Comparatively, the Goldstone mode is more robust to the effect of disorder. However, for sufficiently strong disorder, the Goldstone mode no longer has a well defined dispersion relation. This translates into a much broader subgap frequency distribution that makes more difficult its identification.

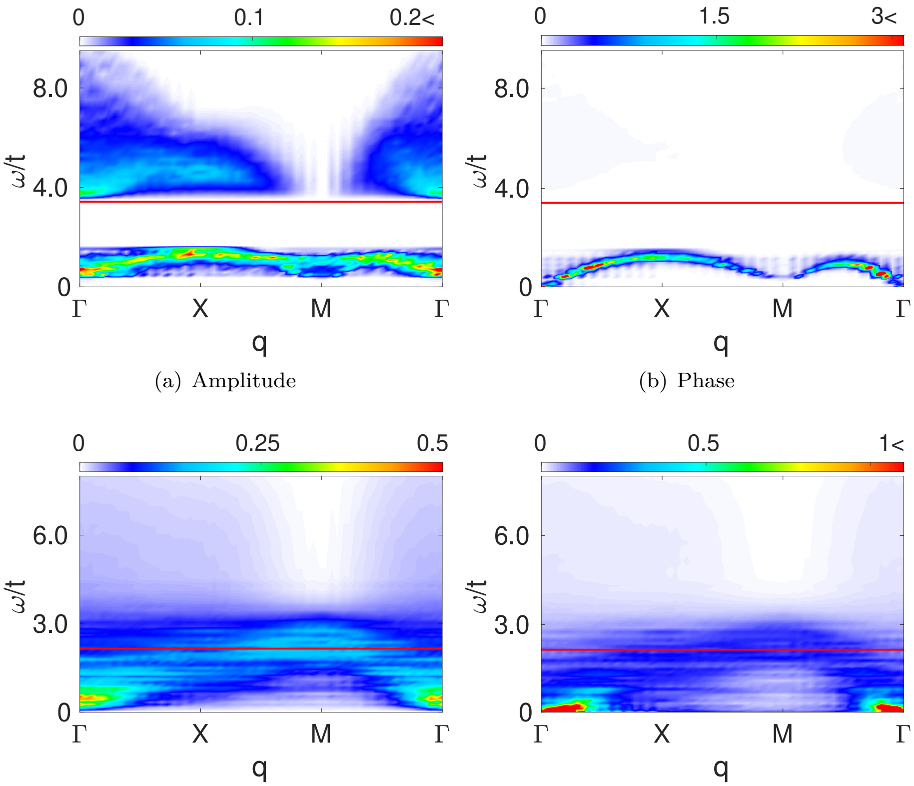

(a) Amplitude (b) Phase

(c) Amplitude (d) Phase

Figure S3. Amplitude ($P^A(q,\omega)$) and phase ($P^\Phi(q,\omega)$) spectral functions for $U = 5$ as a function of momenta q for two values V of disorder. The upper panel is for weak disorder $V = 0.25$ while the lower panel is for intermediate disorder $V = 1.5$. The red horizontal line corresponds to the two-particle spectral gap ω_g. The system size is 20×20 and the average density is $\langle n \rangle = 0.875$.

III. FLUCTUATION CORRELATION FUNCTIONS AND OPTICAL CONDUCTIVITY

In this section we expand the results presented in the main text for the conductivity and the different fluctuation correlation functions. In Fig. S4(a), we present results for the amplitude fluctuation correlation function $C(r) = \langle \tilde{\chi}^{AA}(r,\omega)\rangle / \langle \tilde{\chi}^{AA}(0,\omega)\rangle$ in the clean limit. The correlation function of amplitude fluctuations decays to 0 monotonously with a rather short typical length which suggests that its role in the conductivity is limited.

Likewise, we present results for the phase fluctuation correlation function $C(r) = \langle \tilde{\chi}^{\Phi\Phi}(r,\omega)\rangle / \langle \tilde{\chi}^{\Phi\Phi}(0,\omega)\rangle$ in Fig. S4(b) and S4(c) for two different couplings U. The behavior of the phase fluctuation correlation function is more interesting. We observe damped oscillations around $C(r) = 0$ with increasing distance where the excitation energy is always below the two-particle spectral gap. In the strong coupling limit $U = 5$, we observe a rich oscillating pattern of damped oscillations in $C(r)$ starting at relatively small frequencies $\omega \gtrsim 0.04\omega_g$ and covering a relatively broad range of subgap energies.

Finally, we compute the optical conductivity in a similar range of parameters. For $U = 5$, results depicted in in Fig. S5(a), indicate a subgap peak $\omega \sim 0.18\omega_g$ with some broadening even for weak disorder $V = 0.25$. As disorder increases, the peak becomes broader and shifts to larger energies. For intermediate coupling, $U = 2$ and $\langle n \rangle = 0.875$ we observe qualitatively similar results. Even for weak disorder $V = 0.26$, we still observe a well defined subgap peak albeit at larger frequencies $0.6\omega_g$, see Fig. S5(b). As in the strong coupling region, the peak becomes broader and disorder increases.

We stress that these results in stark contrast with the weak coupling region investigated in the main text for which a subgap excitation only occurs for much stronger disorder.

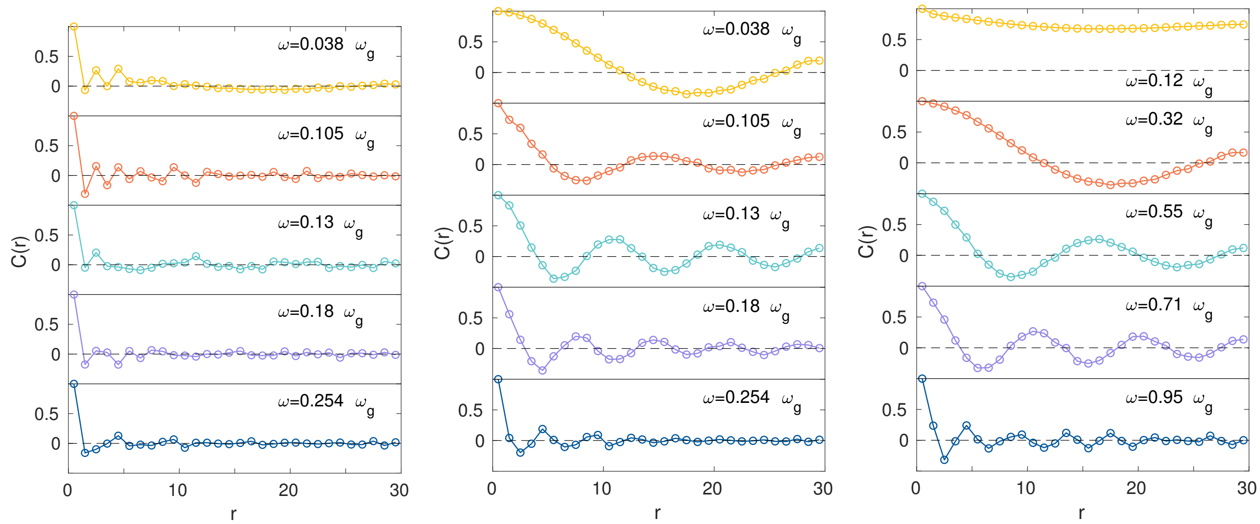

(a) Amplitude (b) Phase (c) Phase

Figure S4. (a). The amplitude fluctuation correlation function in the strong coupling limit $U = 5$. (b) and (c) are the phase fluctuation correlations. (b) is also for $U = 5$, while (c) is for intermediate coupling $U = 2$. The other parameters are $V = 0, L = 30$, and $\langle n \rangle = 0.875$.

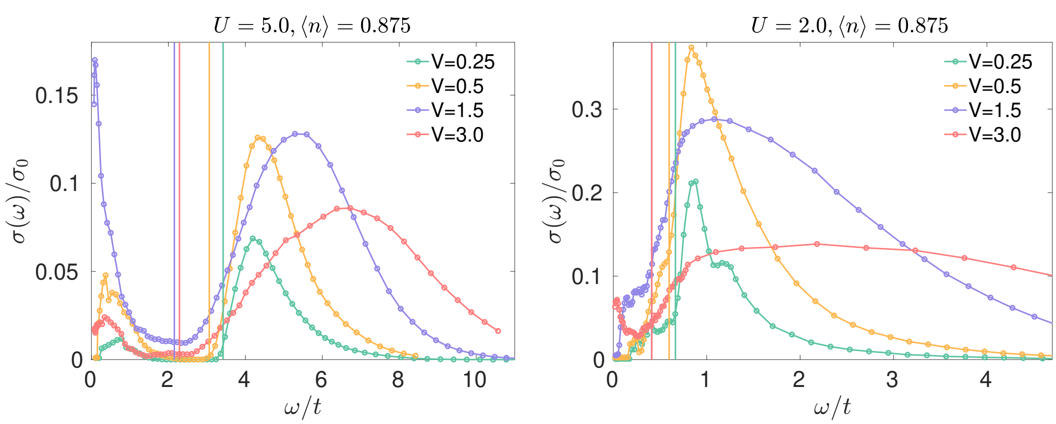

(a) (b)

Figure S5. The optical conductivity $\sigma(\omega)$ in units of $\sigma_0 = \frac{e^2}{\hbar}$. The vertical coloured lines are the corresponding two-particle gaps ω_g.

* bo.fan@sjtu.edu.cn

† abhiseks@campus.technion.ac.il

‡ amgg@sjtu.edu.cn

[1] P. de Gennes, Boundary Effects in Superconductors, Rev. Mod. Phys. **36**, 225 (1964).
[2] P. de Gennes, Superconductivity of Metals and Alloys (W.A. Bebjamin, inc., New York, 1966).
[3] A. Ghosal, M. Randeria, and N. Trivedi, Inhomogeneous pairing in highly disordered s-wave superconductors, Phys. Rev. B **65**, 014501 (2001).
[4] A. Ghosal, M. Randeria, and N. Trivedi, Role of spatial amplitude fluctuations in highly disordered *s*-wave superconductors, Phys. Rev. Lett. **81**, 3940 (1998).
[5] T. Cea, D. Bucheli, G. Seibold, L. Benfatto, J. Lorenzana, and C. Castellani, Optical excitation of phase modes in strongly disordered superconductors, Phys. Rev. B **89**, 174506 (2014).
[6] A. Samanta, A. Ratnakar, N. Trivedi, and R. Sensarma, Two-particle spectral function for disordered *s*-wave superconductors: Local maps and collective modes, Phys. Rev. B **101**, 024507 (2020).